Electronics and Information Technologies, 2026, 34, 225–238
http://publications.lnu.edu.ua/collections/index.php/electronics/index

UDC 535.323, 535.53, 537.226, 548

ELASTIC PROPERTIES OF $RbNH_4SO_4$ CRYSTALS

***Oleh Markevych*[1], *Vasyl Stadnyk*[1], *Oleh Bovgyra*[1], *Roman Lys*[2]*, *Igor Matviishyn*[2], *Oleh Onufriv*[3]**
Ivan Franko National University of Lviv.
[1]Faculty of Physics, 19 Drahomanova St., Lviv, 79005, Ukraine
[2]Faculty of Electronics and Computer Technologies,
107 Henerala Tarnavskoho St., Lviv, 79017, Ukraine
[3]Ukrainian National Forestry University,
103 Henerala Chuprynky St., Lviv, 79057, Ukraine

Markevych, O., Stadnyk, V., Bovgyra, O., Lys, R., Matviishyn, I., & Onufriv, O. (2026). Elastic Properties of $RbNH_4SO_4$ Crystals. *Electronics and Information Technologies*, 34, 225–238. https://doi.org/10.30970/eli.34.15

ABSTRACT

Background. The elastic properties of a material are of great importance in solid-state physics, as they significantly influence the optical properties of crystals.

Materials and Methods. The elastic properties of rubidium ammonium sulfate ($RbNH_4SO_4$) crystals are investigated in this work. The calculation of elastic properties was carried out using the CASTEP program.

Results and Discussion. Analysis of the elastic coefficients matrix of $RbNH_4SO_4$ reveals that this crystal belongs to the rhombic system with pronounced elastic anisotropy. The crystal is mechanically stable, with the greatest rigidity along the *Y*–direction and the smallest along the *X*–direction. The most stable shear is in the *XZ* plane, and the least stable is in the *XY* plane. The calculation of the Cauchy relations revealed a significant deviation ($C_{ij} > C_{kl}$), indicating the predominance of non-central forces in interatomic interaction and a significant contribution of the covalent or ionic component of the bond in the $RbNH_4SO_4$ lattice.

The spatial distributions of Young's modulus, Young's modulus under universal compression, shear modulus, and Poisson's ratio were calculated. The degree of anisotropy in the elastic properties of the $RbNH_4SO_4$ crystal was estimated, confirming its significant anisotropy.

Conclusion. The Born criteria calculation showed that the crystal is mechanically stable. The calculation of the Cauchy relations revealed the predominance of non-central forces in the interatomic interaction and the presence of a significant contribution of the covalent or ionic component of the bond in the $RbNH_4SO_4$ lattice.

The presence of rigid tetrahedral groups $[SO]_4^{2-}$ causes the formation of covalent directed bonds within these groups. It is shown that the polarizability of ions is important: rubidium ions (Rb^+) and sulfate groups $[SO]_4^{2-}$ have large electron shells that deform during mechanical compression of the crystal. This leads to the formation of induced dipole moments. The complex nature of the forces in the $RbNH_4SO_4$ crystal is a consequence of the fact that the crystal consists not of point charges, but of polarizable ions and molecular complexes $[SO]_4^{2-}$ with their own internal covalent bond. This makes the material elastically anisotropic and sensitive to the direction of the applied load.

Keywords: crystal, anisotropy, elastic coefficients, Young's modulus, universal compression modulus, Poisson's ratio.

INTRODUCTION

The refractive indices n_i (RI) and birefringence Δn_i are among the most important optical parameters of materials in the spectral region of transparency. Along with their wide technical application in instrument-making and optoelectronics (information recording, transmission, and storage systems, spatial control of light beams, high-precision polarimetry devices), they are widely used as an effective tool for studying physical processes in crystals. In particular, they allow analyzing the features of electronic polarization, determining the contributions of various effects (thermo-optical, piezo-optical, electro-optical, acousto-optical, etc.) to changes in optical properties, estimating the magnitude of spontaneous polarization and anti-polarization, and investigating their changes during phase transitions. One of the newest applications of their application is biomedicine (for example, studying the microscopic structure of collagen fibers in connective tissue) [1-12].

This research allows us to study piezo- and electro-optical effects, electro- and piezogyration, spatial modulation phenomena, acousto-optic interaction, and photorefraction. It's noteworthy that the optical properties of crystals are closely related to their elastic characteristics. Deformations of the crystal lattice, which arise under the action of mechanical stresses, temperature, or external fields, lead to a change in electronic polarizability and, accordingly, to a change in the refractive indices. This is the basis for the piezo-optical and photoelastic effects, which establish a direct connection between the material's optical and elastic parameters. Therefore, for a thorough understanding of optical characteristics, it is necessary to consider the anisotropy and the values of the elastic constants of crystals, which determine the lattice's response to external influences [13-21].

This article considers the elastic properties of rubidium ammonium sulfate (RAS), $RbNH_4SO_4$ crystals. Previously, the temperature- and spectral-dependence of the main RIs in these crystals was studied. It was established that in the studied spectral region (300–800 nm) and temperature interval (77–820 K), the dispersion $n_i(\lambda)$ is normal and is well described by the two-oscillator Sellmeier formula. The intersection of the dispersion curves $n_i(\lambda)$ in the *Y*-direction was found. The refractions, electronic polarizabilities, and parameters of effective ultraviolet and infrared oscillators were calculated. A 2nd-order phase transition was observed at T = 120 K in the $RbNH_4SO_4$ crystal.

The band-energy structure of $RbNH_4SO_4$ crystals was calculated, and it was found that the top of the valence band of these crystals is localized at point D (**k** = {0.5; 0.5; 0}), the bottom of the conduction band is at point Γ (E = 5.16 eV), and the smallest direct band gap (point Γ) is 5.33. The top of the valence band is formed by the bonding *p*-orbitals of sulfur and oxygen. The bottom of the conduction band is mainly formed by the *s*- and *p*-states of NH_4 and Rb, hybridized with the antibonding *p* states of sulfur and oxygen. It was found that the band gap width of $RbNH_4SO_4$ crystals decreases with increasing pressure ($dE_g / d\sigma \sim -1.55 \cdot 10^{-5}$ eV/bar) [22-25].

Despite the considerable amount of available information regarding the optical and electronic properties of $RbNH_4SO_4$ crystals, their elastic characteristics remain practically unexplored. This lack of information significantly limits a comprehensive understanding of the coupling between mechanical deformation and optical response in these materials. Elastic properties are among the fundamental characteristics of crystalline solids because they determine the propagation of acoustic waves, mechanical stability, energy transfer processes, thermal transport, and the response of a crystal to external mechanical loading. In anisotropic crystals, the elastic response strongly depends on crystallographic direction, resulting in elastic anisotropy that plays a crucial role in many physical phenomena.

The study of elastic anisotropy has become particularly important in recent years due to the rapid development of acoustic metamaterials, phononic crystals, and anisotropic functional media. Modern materials science increasingly focuses on designing materials with highly anisotropic elastic properties, enabling unprecedented control over the

propagation of elastic and acoustic waves. Such materials can be employed for acoustic waveguiding, vibration suppression, sound insulation, acoustic cloaking, and advanced signal-processing systems. Elastic anisotropy also governs the directional dependence of sound velocities, acoustic attenuation, and acousto-optic interaction efficiency, making it a key parameter for the development of modern acoustic and photonic technologies.

From the viewpoint of crystal optics, elastic anisotropy is directly related to photoelastic, piezo-optic, and acousto-optic phenomena. Mechanical deformations modify the dielectric tensor of a crystal through the photoelastic effect, thereby changing its refractive indices and birefringence. Consequently, knowledge of the elastic tensor is indispensable for understanding and predicting the optical response of crystals under external stress. This is particularly important for materials that may serve as active elements of optical modulators, deflectors, polarization controllers, and optical sensing devices.

The mixed-cation nature of $RbNH_4SO_4$ crystals makes them especially interesting for elastic investigations. The coexistence of relatively large Rb^+ ions and orientationally active NH_4^+ groups creates a complex system of interatomic interactions, which may result in pronounced anisotropy of the elastic tensor. The presence of rigid $[SO]_4^{2-}$ tetrahedra combined with comparatively flexible cation sublattices is expected to generate anisotropic deformation mechanisms associated with both translational displacements of cations and rotational distortions of sulfate tetrahedra. Therefore, the analysis of elastic anisotropy can provide valuable insight into the microscopic nature of interatomic bonding and structural stability in these crystals.

In view of these considerations, the present work is devoted to a comprehensive investigation of the elastic properties of $RbNH_4SO_4$ crystals. Special attention is focused on the determination of the elastic stiffness coefficients, evaluation of the mechanical stability conditions, analysis of elastic anisotropy, and discussion of the relationship between elastic behavior, crystal structure, and optical characteristics. The obtained results are expected to contribute to a deeper understanding of the mechanical and acousto-optic properties of $RbNH_4SO_4$ crystals and to assess their potential for applications in modern optical and acoustic devices.

MATERIALS AND METHODS

The elastic properties of the $RbNH_4SO_4$ crystal were calculated using the CASTEP program, based on density functional theory (DFT) [26-32]. This technique combines the pseudopotential approach with plane waves, which makes it fast and widely used in solid-state chemistry and physics. The following electronic configurations were used for the valence electrons: O ($1s^2\ 2s^2\ 2p^4$); S ($1s^2\ 2s^2\ 2p^6\ 3s^2\ 3p^4$), N ($1s^2\ 2s^2\ 2p^3$), H ($1s^1$), Rb ($4s^2\ 4p^6\ 5s^1$). The ionic core was described using a norm-conserving pseudopotential [29], and the limiting kinetic energy controlling the number of plane waves was taken to be E_{cut} = 750 eV. Integration over the 1st Brillouin zone was performed at points of a 3×2×4 k-grid selected by the Monkhorst-Pack scheme [30].

To describe quantum exchange and correlation effects, the local density approximation (LDA) and the generalized gradient approximation (GGA) with the Perdew-Burke-Ernzerhof (PBE) parameterization were initially considered [31, 32]. As is well known, the use of the LDA functional typically leads to an underestimation of lattice parameters (by 1–3 %), resulting in a significant overestimation of elastic moduli and elastic coefficients C_{ij} (sometimes up to 10–20 % compared to experimental data). Conversely, the PBE functional tends to overestimate lattice parameters (by 1–2 %), which leads to a systematic underestimation of the elastic constants. Therefore, the PBEsol functional [33] was employed to ensure a precise balance between the cell geometry and the strain-energy relation. The PBEsol functional, specifically adapted for solids, provides a well-balanced description of the potential energy surface and yields elastic constants C_{ij} that lie between the LDA and PBE results. PBEsol is recognized as one of the most accurate and

well-balanced approximations for minimizing systematic errors in the calculation of elastic properties, as it delivers results comparable to those obtained from much more computationally expensive hybrid functionals, such as HSE and PBE0 [34,35].

The optimization procedure was performed similarly to works [36-38] with the following convergence criteria: maximum force $3 \cdot 10^{-2}$ eV/Å; maximum stress $5 \cdot 10^{-3}$ GPa; maximum atomic displacement $1 \cdot 10^{-4}$ Å. To calculate the elastic properties of the $RbNH_4SO_4$ crystal, known crystallographic data for this crystal with the space symmetry group No. 2 (P_{nam}) were used (**Table 1**). The results of the lengths and occupancy degrees of the shortest atomic bonds of this crystal are also given there.

Table 1. **Crystal lattice parameters, length, and degree of occupancy of the shortest atomic bonds in the rubidium-ammonium sulfate crystal**

Parameter	Experiment	Calculation
a, Å	7.830	7.696
b, Å	10.467	10.368
c, Å	5.977	5.932
V, Å^3	489.855	473.326
Z	4	4
Bond	**Length (Å)**	**Occupancy**
N–H	1.028–1,051	0.85–0.78
S–O	1.459–1,492	0.67–0.56
H–H	1.655–1,725	from –0.10 to –0.09
O–H	1.746–2,705	from 0.11 to –0.01
O–O	2.410–2,434	from –0.24 to –0.23
S–H	2.610–2,665	–0.03
N–O	2.796–2,935	from –0.14 to –0.04
Rb–O	2.867	0.08

The elastic properties are described by Hooke's law, which is written as follows for anisotropic materials [13, 39]:

$$\sigma_{mk} = C_{mknl}\varepsilon_{nl}, \tag{1}$$

where σ_{mk} is the stress tensor, C_{mknl} is the elastic coefficients, and ε_{nl} is the strain tensor. The $RbNH_4SO_4$ crystal belongs to the orthorhombic symmetry class. From a symmetry point of view, the elastic coefficients of such a crystal form a symmetric 6×6 matrix (in Voigt notation) containing 12 nonzero components, nine of which are independent: C_{11}, C_{22}, C_{33}, C_{44}, C_{55}, C_{66}, C_{12}, C_{13}, and C_{23}.

The coefficients C_{ij} were obtained by expanding the total energy $E(V, \delta)$ of the crystal in a Taylor series with respect to the unit cell volume V. For small deformations ($\delta \ll 1$), the energy per unit volume is described as follows [39]:

$$E(V, \delta) = E(V_0, 0) + V_0 \sum_{i=1}^{6} \sigma_i \, e_i + \frac{V_0}{2} \sum_{i,j=1}^{6} C_{ij} e_i e_j \,, \tag{2}$$

where V_0 is the equilibrium volume at zero pressure; e_i are the components of the deformation tensor in Voigt notation; C_{ij} are the second-order elastic coefficients, which are defined as the curvature of the energy surface:

$$C_{ij} = \frac{1}{V_0}\left[\frac{\partial^2 E}{\partial e_i \partial e_j}\right]. \quad (3)$$

Here, a set of strain tensors is used to calculate all 9 coefficients. Each strain δ causes an energy change $\Delta E = E(\delta) - E(0)$, which is a quadratic function of δ. Tensile/compressive strains along the axes are used to calculate the longitudinal and transverse moduli C_{ij}.

As an example, in the case of strain along the *X* axis ($e = \{\delta, 0, 0, 0, 0, 0\}$), it is obtained that:

$$\frac{\Delta E}{V_0} = \frac{1}{2} C_{11}\delta^2. \quad (4)$$

For orthogonal deformation (*XY* plane), we will have $e = \{\delta, -\delta, 0, 0, 0, 0\}$, which will correspond to the relation:

$$\frac{\Delta E}{V_0} = (C_{11} + C_{22} - 2C_{12})\delta^2/2. \quad (5)$$

Using the coefficients C_{11} and C_{22}, the coefficient C_{12} can be calculated. To calculate the shear moduli (C_{44}, C_{55}, C_{66}), shear deformations with volume conservation were used. In the case of shear in the *YZ* plane ($e = \{0, 0, 0, \delta, 0, 0\}$) we can write:

$$\frac{\Delta E}{V_0} = \frac{1}{2} C_{44}\delta^2. \quad (6)$$

Similar expressions can be written for the coefficients C_{55} (displacement in the *XZ* plane) and C_{66} (displacement in the *XY* plane). For calculations of the bulk modulus *B*, it is taken into account that the crystals of the rhombic syngony are related to the elastic moduli C_{ij} by the formula:

$$B = \frac{1}{9}\{C_{11} + C_{22} + C_{33} + 2(C_{12} + C_{13} + C_{23})\}. \quad (7)$$

Poisson's ratios (V_{ij}), which show the transverse compression of the crystal in the *j* direction during its stretching along the *i* direction, were calculated using the following formulas:

$$V_{XY} = -\frac{C_{11}}{C_{12}},\ V_{XZ} = -\frac{C_{11}}{C_{13}},\ V_{YZ} = -\frac{C_{22}}{C_{23}},$$
$$V_{YX} = -\frac{C_{22}}{C_{21}},\ V_{ZX} = -\frac{C_{33}}{C_{31}},\ V_{ZY} = -\frac{C_{33}}{C_{32}}. \quad (8)$$

Using the elastic coefficient matrix, the spatial distribution of Young's modulus is calculated in the work. For this, first, the inverse matrix of elastic compliance coefficients $[S] = [C]^{-1}$ is found. Then the Young's modulus E in the direction given by the unit vector $\mathbf{n} = [l_1, l_2, l_3]$ (where l_i are the direction cosines relative to the crystallographic axes) is calculated by the general formula:

$$\frac{1}{E} = \sum_{i=1}^{3}\sum_{j=1}^{3}\sum_{k=1}^{3}\sum_{l=1}^{3} S_{ijkl} l_i l_j l_k l_l. \tag{9}$$

RESULTS AND DISCUSSION

The matrix of elastic coefficients C_{ij} (GPa) of the $RbNH_4SO_4$ crystal at room temperature looks like

$$\mathbf{C} = \begin{bmatrix} 17.45 & 6.05 & 5.87 & 0 & 0 & 0 \\ 6.05 & 19.56 & 5.54 & 0 & 0 & 0 \\ 5.87 & 5.52 & 17.88 & 0 & 0 & 0 \\ 0 & 0 & 0 & 5.24 & 0 & 0 \\ 0 & 0 & 0 & 0 & 6.78 & 0 \\ 0 & 0 & 0 & 0 & 0 & 4.86 \end{bmatrix}. \tag{10}$$

We see that the matrix with nine independent non-zero components is characteristic of rhombic symmetry. In the given case, an approximation to tetragonal symmetry is observed, since $C_{11} \approx C_{33}$ (17.45 ≈ 17.88 GPa) and $C_{44} \approx C_{66}$. However, the difference between C_{22} and the components $C_{12} \neq C_{13}$ confirms the rhombic structure.

The rubidium ammonium sulfate (RAS) crystal $RbNH_4SO_4$ belongs to the orthorhombic system (space group of type P_{nma}); therefore, its tensor of elastic coefficients contains 9 independent components C_{ij}, which are given in Eq. (10). Regarding the shear stiffness, it can be noted that the shear resistance is maximum in the *XZ* plane (C_{55} = 6.78 GPa) and minimum and almost isotropic in the *YZ* and *XY* planes ($C_{44} \approx C_{66}$).

For a stable crystal, the Born conditions must be fulfilled. For crystals of the rhombic system, the Born conditions of mechanical stability are written as follows:

$$\begin{aligned} &C_{11} > 0, C_{22} > 0, C_{33} > 0, C_{44} > 0, C_{55} > 0, C_{66} > 0; \\ &[C_{11} + C_{22} + C_{33} - 2(C_{12} + C_{13} + C_{23})] > 0; \\ &(C_{11} + C_{22} - 2C_{12}) > 0; \quad (C_{11} + C_{33} - 2C_{13}) > 0; \quad (C_{22} + C_{33} - 2C_{23}) > 0. \end{aligned} \tag{11}$$

The check showed that

$$\begin{aligned} &C_{11} + C_{22} - 2C_{12} = 17.45 + 19.56 - 2 \cdot 6.05 = 24.91 > 0; \\ &C_{11} + C_{33} - 2C_{13} = 17.45 + 17.88 - 2 \cdot 5.87 = 23.59 > 0; \\ &C_{22} + C_{33} - 2C_{23} = 19.56 + 17.88 - 2 \cdot 5.54 = 26.36 > 0; \\ &C_{11} + C_{22} + C_{33} + 2(C_{12} + C_{13} + C_{23}) = 54.89 + 2 \cdot 17.46 = 89.81 > 0. \end{aligned}$$

We see that all the criteria are met, so the crystal is mechanically stable. Let us compare the main elastic coefficients. Since $C_{22} > C_{33} > C_{11}$, the greatest stiffness is along the *b*-direction, while along the *a*-direction it is the least. That is, the *b*-direction is the stiffest, and the *a*-direction is the most compressible. This is a typical result for crystals of

the $ABSO_4$ double sulfate family (A and B = Li, K, Na, Cs, Rb, and NH_4), in which stiffer polyhedral SO_4 chains form along one axis. Since $C_{55} > C_{44} > C_{66}$, the most stable shear is in the *XZ* plane, while in the *XY* plane it is the least stable. This may be due to weaker interionic interactions between layers or to the orientational mobility of NH_4^+ groups.

An important indicator is the deviation from the Cauchy relations ($C_{12} = C_{66}$, $C_{13} = C_{55}$, $C_{23} = C_{44}$). From the matrix, we see that C_{12} (6.02) ≠ C_{66} (4.86) and C_{23} (5.54) ≠ C_{44} (5.24). A significant deviation ($C_{ij} > C_{kl}$) indicates the predominance of non-central forces in the interatomic interaction and the presence of a significant contribution of the covalent or ionic component of the bond in the $RbNH_4SO_4$ lattice.

Analysis of the matrix shows that the $RbNH_4SO_4$ crystal belongs to the rhombic syngony with pronounced elastic anisotropy (maximum stiffness along the *Y* axis). The inequality in the elastic constants indicates the complex nature of interatomic forces, which extend beyond simple central interactions. This "violation" means that the real interaction in rubidium ammonium sulfate is much more complex.

The reason for the “complex nature” of the forces in $RbNH_4SO_4$ is the presence of rigid tetrahedral groups $[SO]_4^{2-}$. The bonding within these groups is covalent, meaning there are directional bonds. Unlike ionic bonding, which acts equally in all directions, directional bonds resist changes in the angles between atoms, not just changes in distance. This creates “angular” or “multi-particle” forces that do not fit into the model of simple central springs.

The ions' polarizability also plays an important role. The rubidium ions Rb^+, ammonium ions NH_4^+, and, especially, the sulfate groups $[SO]_4^{2-}$ have large electron shells that deform during mechanical compression of the crystal. In the case of crystal compression, induced dipole moments arise. The “dipole-dipole” interaction depends on the orientation, which again adds an off-center component to the total lattice energy.

From the matrix, we also see that, since the Cauchy parameter $g=C_{12}-C_{44}=6.05-5.24>0$, this indicates the predominance of ionic character with pronounced polarizability. The crystal resists a change in volume (compression) more than a change in shape (shear). This is a consequence of the fact that interatomic forces “hold” the structure not only due to electrostatic attraction, but also due to the rigid geometry of sulfate groups. That is, the complex nature of the forces in the $RbNH_4SO_4$ crystal is a consequence of the fact that the crystal consists not of point charges, but of polarizable ions and molecular complexes $[SO]_4^{2-}$ with their own internal covalent bond. This makes the material elastically anisotropic and sensitive to the direction of the applied load.

For orthorhombic crystals, the maxima of Young's modulus are usually close to the crystallographic axes. If we compare the diagonal components of the stiffness tensor: $C_{22}>C_{33}>C_{11}$, it follows that the maximum Young's modulus is along the b axis, along the c axis it is slightly smaller, and along the a axis it is minimal. That is, the indicatrix of Young's modulus should be elongated along the b axis. Physically, this means that the crystal is stiffest in the b direction, and deformation occurs most easily along the a direction. Since the coefficients of the shear moduli satisfy the following relationship: $C_{55}>C_{44}>C_{66}$, this means that the lowest shear resistance is in the plane (ab). In a spatial surface, this manifests itself as a flattening of the indicatrix (**Fig. 1a**).

Poisson's ratio, *ν*, is one of the fundamental characteristics of the elastic properties of solids. It describes the mechanical coupling between longitudinal and transverse deformations of a load. If a uniaxial tensile stress *σ* is applied to a body, it elongates along the direction of the load and simultaneously compresses in the transverse directions. Poisson's ratio ν is given by the formula:

$$\nu = -\frac{\varepsilon_{\perp}}{\varepsilon_{\parallel}}, \tag{12}$$

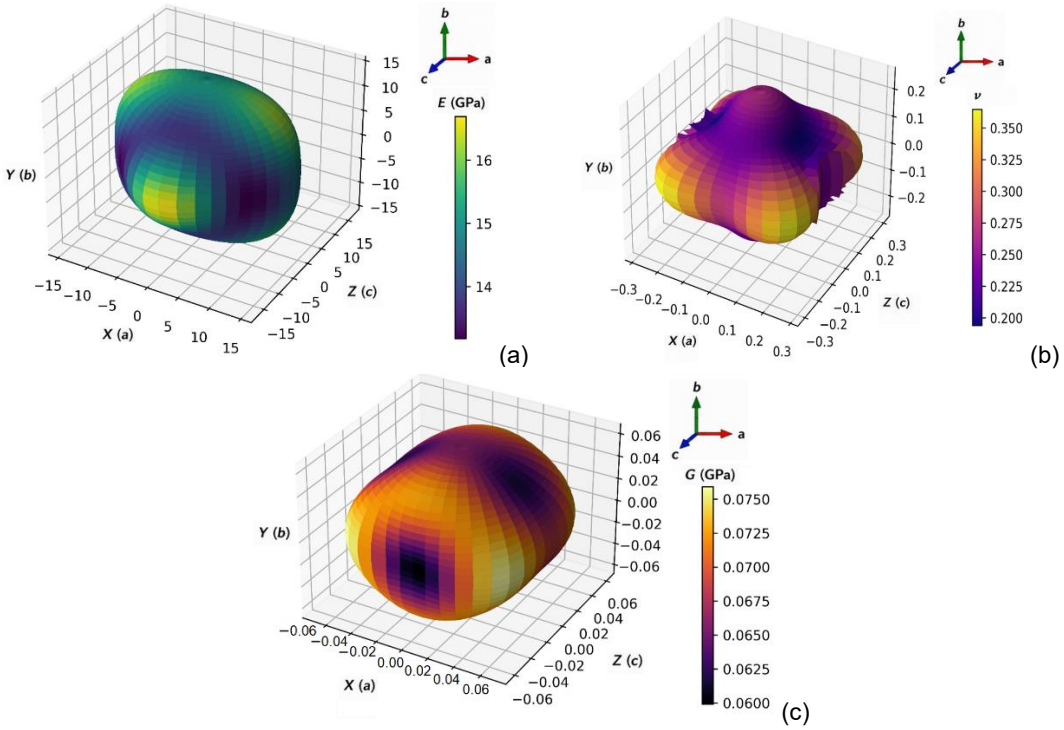

Fig. 1. Spatial distribution of Young's modulus (a), Poisson's ratio (b), and linear compressibility (c) of the $RbNH_4SO_4$ crystal at room temperature

where $\varepsilon_{\parallel}$ is the relative longitudinal strain, and $\varepsilon_{\perp}$ is the transverse strain. The minus sign in the formula means that the strains have opposite signs.

For most dielectric crystals, $\nu \approx 0.2–0.3$, which agrees well with the values obtained for the $RbNH_4SO_4$ crystal (**Fig. 1b**). In anisotropic crystals, ν is not a constant. It depends on the direction of the applied stress $\mathbf{n}$ and the direction of the transverse strain $\mathbf{m}$. Therefore, 3D Poisson's ratio surfaces or polar sections are constructed for crystals in certain crystallographic planes. In some directions, the value may differ significantly.

For an anisotropic crystal

$$\nu(\mathbf{n}, \mathbf{m}) = -\frac{s_{ijkl} n_i n_j m_k m_l}{s_{ijkl} n_i n_j n_k n_l}, \tag{13}$$

where s_{ijkl} is the compliance tensor, $\mathbf{n}$ is the load direction, and $\mathbf{m}$ is the direction of transverse deformation. This formula is used to construct spatial maps of ν.

For the $RbNH_4SO_4$ crystal, Poisson's ratio reflects the rigidity of the SO_4 tetrahedra, the relatively soft deformations of the NH_4^+ ion, and the weak participation of the Rb^+ ions in covalent bonding. This leads to moderate values of v and anisotropy of transverse deformations.

Poisson's ratio determines the propagation of acoustic waves, acousto-optic effects, the material's behavior under pressure, and the mechanical stability of the crystal. Therefore, its analysis is an important part of the study of the elastic and optical properties of crystals.

Poisson's ratio determines the transverse strain during tension. Since the off-diagonal coefficients C_{12}, C_{13}, and $C_{23} \approx 5.5–6.0$ GPa, are not significant enough, there is little transverse interaction between the axes in the crystal. Values of approximately $\nu \approx 0.18–$

0.30, maxima occur in directions close to the (*ab*) and (*ac*) planes, where shear strains are lighter.

Anisotropy in $RbNH_4SO_4$ is determined by its lattice structure: the rigid structural elements of the SO_4 tetrahedra are held together by strong covalent bonds. The softer elements, the NH_4^+ ion, form hydrogen bonds that are much softer. The weakly bound Rb^+ cation is mainly ionically bound. Therefore, there is great rigidity along the directions of the SO_4 chains, and there are lighter deformations in the directions involving NH_4.

The obtained surfaces (**Fig. 1c**) indicate moderate elastic anisotropy and have pronounced directions of light shear. This is important for piezo-optical effects, baric changes in refractive indices, and acousto-optical properties.

Compared to the isomorphic Rb_2SO_4 crystal, $RbNH_4SO_4$ usually exhibits lower shear moduli and higher anisotropy. The reason is the presence of the NH_4 ion, which reduces the coefficients due to orientational degrees of freedom. The main rigidity of the $RbNH_4SO_4$ crystal is formed by SO_4 tetrahedra. Such properties are in good agreement with phase transitions, anisotropy of thermal expansion, and anisotropy of thermo-optic coefficients dn/dT.

Thus, the $RbNH_4SO_4$ crystal has mechanical stability, moderate anisotropy of longitudinal moduli, significant anisotropy of shear deformations, and a relatively small bulk modulus (~10 GPa). Such properties are typical for ionic-molecular sulfate crystals with SO_4 tetrahedra and orientationally mobile NH_4 groups.

Young's modulus characterizes the rigidity of the material during uniaxial tension or compression. In crystals, the strain depends on the orientation of the load relative to the crystallographic axes. Therefore, the directional Young's modulus $E(\theta, \varphi)$ is introduced, where θ and φ are spherical angles that define the direction in the crystal. The Young's modulus was calculated using formula (9).

The dependence $E(\theta, \varphi)$ is usually depicted as a three-dimensional surface. In each direction, the radius r=$E(\theta, \varphi)$ is plotted. The resulting surface is called the Young's modulus indicatrix. Its shape characterizes the degree of elastic anisotropy and the directions of maximum and minimum stiffness. For isotropic materials, this surface is a sphere $E(\theta, \varphi)$=$const$, for weakly anisotropic crystals, it is close to an ellipsoid, and for strongly anisotropic crystals, elongated petal structures or directions with very small E may occur. In most crystals, the maximum of Young's modulus corresponds to the directions of the strongest chemical bonds or the densest packing of atoms. The directions of weak interionic bonds or possible slip planes correspond to the minimum value.

It is known that the structure of the $RbNH_4SO_4$ crystal is determined by SO_4 tetrahedra, Rb^+ cations, and NH_4^+ groups. The rigidity of the lattice is determined by strong covalent S–O bonds, ionic bonds with the Rb atom, and rather weak NH_4 hydrogen interactions. Therefore, Young's modulus has maxima along the directions where the SO_4 tetrahedra are more tightly connected, and minima in the directions where deformation occurs due to rotation or displacement of the NH_4 groups.

The Young's modulus is related to the bulk modulus B, the shear modulus G, and the Poisson's ratio ν by the following relationship (isotropic case): E=$9BG/(3B$+$G)$. Therefore, the spatial distribution of Young's modulus E is a combination of the shear stiffness and compressibility of the crystal. The shear anisotropy of crystals of the orthorhombic system is characterized by the following coefficients:

$$A_1 = \frac{4C_{44}}{C_{11} + C_{33} - 2C_{13}};\ A_2 = \frac{4C_{55}}{C_{11} + C_{22} - 2C_{12}};\ A_3 = \frac{4C_{66}}{C_{22} + C_{33} - 2C_{23}}. \quad (14)$$

If we substitute the values from Eq. (10) into these ratios, we can obtain the following values: $A_1 \approx 1.82$, $A_2 \approx 2.16$, and $A_3 \approx 1.03$. If $A = 1$, then there is isotropic behavior,

and if $A \neq 1$, then there is anisotropic behavior. Therefore, the greatest anisotropy is in the plane (*ac*), and the least is in the plane (*bc*).

Since $C_{22} > C_{33} > C_{11}$, we can estimate that $E_b > E_c > E_a$. That is, the maximum stiffness is along the b axis, the minimum along the a axis. The approximate ratio $E_{max}/E_{min} \approx 1.3 - 1.4$, which corresponds to moderate elastic anisotropy.

For the general characteristic, the parameter is used:

$$A^U = 5\frac{G_V}{G_R} + \frac{B_V}{B_R} - 6, \quad (15)$$

where G_V, B_V are Voith estimates, G_R, B_R are Reis estimates. For our set of constants, we obtain approximately $A^U \approx 0.4 - 0.6$. If $A = 0$, then there is practically no anisotropy, and if $A = 0..1$, then there is weak or moderate anisotropy. Thus, for the $RbNH_4SO_4$ crystal, there is moderate elastic anisotropy.

The structure of $RbNH_4SO_4$ contains rigid SO_4 tetrahedra, the Rb^+ ion, and NH_4^+ groups. The anisotropy arises from the different orientations of the SO_4 tetrahedra, the possibility of NH_4 rotation, and weaker hydrogen bonds. This leads to the fact that deformation occurs more easily in some planes and more difficultly along the directions of tight binding. For the Rb_2SO_4 crystal, the anisotropy is usually slightly smaller. The reason is the absence of the NH_4 molecular group and a more rigid ionic lattice.

CONCLUSION

The elastic properties of $RbNH_4SO_4$ crystals at room temperature have been investigated for the first time using a comprehensive analysis of the elastic stiffness tensor. The obtained results fill an existing gap in literature concerning the mechanical characteristics of this crystal and provide the necessary basis for understanding the coupling between its elastic, optical, and electronic subsystems.

Analysis of the elastic stiffness matrix confirmed that $RbNH_4SO_4$ belongs to the orthorhombic crystal system and exhibits pronounced elastic anisotropy. The inequality of the principal elastic constants ($C_{22} > C_{33} > C_{11}$) indicates that the crystal possesses the highest resistance to uniaxial deformation along the *Y* crystallophysical direction, whereas the *X* direction is mechanically the softest. A substantial anisotropy was also found for shear deformation, with the highest shear stability observed in the *XZ* plane and the lowest in the *XY* plane. These results reveal a strong directional dependence of the interatomic interactions and deformation mechanisms operating in the crystal lattice.

Mechanical stability was confirmed by satisfying all Born stability criteria. At the same time, a significant deviation from the Cauchy relations was established, providing clear evidence for the predominance of non-central interatomic forces. This behavior originates from the coexistence of rigid covalently bonded sulfate tetrahedra and comparatively flexible ionic sublattices formed by Rb^+ and NH_4^+ ions. The obtained results demonstrate that the elastic response of $RbNH_4SO_4$ cannot be described within the framework of simple central-force models and is governed by complex many-body interactions, directional bonding effects, and the intrinsic polarizability of the constituent structural units.

A detailed analysis of the elastic anisotropy revealed that the rigid $[SO]_4^{2-}$ tetrahedra act as the main structural elements controlling the mechanical behavior of the crystal. Under external loading, deformation is primarily accommodated through rotations and distortions of sulfate tetrahedra as well as displacements of Rb^+ and NH_4^+ ions. Such a deformation mechanism gives rise to pronounced anisotropy of the elastic tensor and explains the observed directional dependence of the Young's modulus, shear modulus, compressibility, and Poisson's ratio.

For the first time, three-dimensional spatial distributions of the Young's modulus, linear compressibility, shear modulus, and Poisson's ratio were calculated and analyzed. The resulting surfaces reveal a highly anisotropic mechanical response, which is directly related to the crystal structure and anisotropic arrangement of sulfate groups. The universal elastic anisotropy index was estimated to be $A^U \approx 0.4–0.6$, indicating a moderate-to-high degree of elastic anisotropy. The relatively small difference between the Voigt and Reuss approximations confirms the reliability of the elastic characteristics obtained while simultaneously reflecting the intrinsic anisotropic nature of the crystal.

The results obtained are important not only from a fundamental perspective but also for potential practical applications. Knowledge of the elastic tensor and elastic anisotropy is essential for evaluating the acousto-optic, photoelastic, and piezo-optic properties of $RbNH_4SO_4$ crystals. The pronounced anisotropy of the elastic response suggests the possibility of directional control of acoustic-wave propagation and acousto-optic interaction efficiency. Therefore, $RbNH_4SO_4$ can be considered a promising material for acousto-optic modulators, deflectors, polarization-control elements, and optical sensors operating under external mechanical loading.

Furthermore, the calculated elastic parameters provide a basis for future investigations of acoustic-wave velocities, photoelastic coefficients, acousto-optic figures of merit, and strain-induced modifications of the electronic band structure and refractive characteristics. Consequently, the present study establishes a fundamental framework for the development of multifunctional optical and acoustic devices based on $RbNH_4SO_4$ crystals.

ACKNOWLEDGMENTS AND FUNDING SOURCES

The authors received no financial support for the research, writing, and/or publication of this article.

COMPLIANCE WITH ETHICAL STANDARDS

The authors declare that they have no competing interests.

AUTHOR CONTRIBUTIONS

Conceptualization, [O.M., V.S., O.B.]; methodology, [O.M., O.B., V.S.]; investigation, [O.M., V.S., R.L., I.M., O.O.]; writing – original draft preparation, [O.M., R.L.]; writing – review and editing, [O.M., V.S., O.B., R.L.]; visualization, [O.M., O.B.].

All authors have read and agreed to the published version of the manuscript.

REFERENCES

[1] Goodman, J. W. (2005). *Introduction to Fourier optics*. Roberts & Company Publishers, 491 p.
[2] Flowers, G. R. (2012). *Introduction to modern optics*. Courier Corporation, 352p.
[3] Iizuka, K. (2002). *Elements of photonics: Volume II: For fiber and integrated optics*. John Wiley & Sons, 1222 p. https://doi.org/10.1002/0471221376
[4] Kubby, J. A. (2013). *Adaptive optics for biological imaging*. CRC Press, 388 p. https://doi.org/10.1201/b14898
[5] Goldstein, D. H. (2011). *Polarized light* (3rd ed.). CRC Press, 808 p. https://doi.org/10.1201/b10436
[6] Hao, R., Zeng, N., Zhang, Z., He, H., He, C., & Ma, H. (2024). Polarization feature fusion and calculation of birefringence dynamics in complex anisotropic media. *Optics Letters, 49*(9), 2273. https://doi.org/10.1364/OL.515983
[7] Zhang, Z., Hao, R., Shao, C., Mi, C., He, H., et al. (2023). Analysis and optimization of aberration induced by oblique incidence for in vivo tissue polarimetry. *Optics Letters, 48*(23), 6136–6139. https://doi.org/10.1364/OL.501365

[8] Ghosh, N., & Vitkin, A. (2011). Tissue polarimetry: Concepts, challenges, and applications. *Journal of Biomedical Optics, 16*(11), 110801. https://doi.org/10.1117/1.3652896
[9] Ramella-Roman, J. C., Saytashev, I., & Piccini, M. (2020). A review of polarization-based imaging technologies for clinical and preclinical applications. *Journal of Optics, 22*(12), 123001. https://doi.org/10.1088/2040-8986/abbf8a
[10] Zaffar, M., & Pradhan, A. (2020). Assessment of anisotropy of collagen structures through spatial frequencies of Mueller matrix images for cervical pre-cancer detection. *Applied Optics, 59*(4), 1237–1248. https://doi.org/10.1364/AO.377105
[11] Yang, H., Song, J., Zeng, N., & Ma, H. (2023). Local optimized Stokes polarimetry for specific polarization states. *Optics Letters, 48*(11), 3019–3022. https://doi.org/10.1364/OL.490110
[12] Wang, L., Peng, Y., Zhang, H., & Zhao, C. (2025). Generalized Stokes polarimetry design for a 3D polarization field. *Optics Letters, 50*(2), 293–296. https://doi.org/10.1364/OL.546036
[13] Nye, J. F. (1985). *Physical properties of crystals: Their representation by tensors*. Oxford University Press, 352 p.
[14] Ting, T. C. T. (1996). *Anisotropic elasticity: Theory and applications*. Oxford University Press, 592 p. https://doi.org/10.1093/oso/9780195074475.001.0001
[15] Newnham, R. E. (2005). *Properties of materials: Anisotropy, symmetry, structure*. Oxford University Press, 378 p. https://doi.org/10.1093/oso/9780198520757.001.0001
[16] Waxler, R. M., & Feldman, A. (1980). Optical properties of materials. *Applied Optics, 19*(15), 2481–2489. https://doi.org/10.1364/AO.19.002481
[17] Mytsyk, B. (2003). Methods for the studies of piezooptic effect in crystals and analysis of the experimental data. II. Analysis of the experimental data. *Ukrainian Journal of Physical Optics*, 4(3), 105–110. https://doi.org/10.3116/16091833/4/3/105/2003
[18] Oseledchik, S., Prosvirnin, A., Pisarevskiy, A. I., & others. (1995). Optical properties of anisotropic materials. *Optical Materials, 4*(6), 669–675. https://doi.org/10.1016/0925-3467(95)00027-5
[19] Polian, A., & Grimsditch, M. (1999). Elastic properties under pressure. *Physical Review B, 60*(3), 1468–1473. https://doi.org/10.1103/PhysRevB.60.1468
[20] Chilla, E., Flannery, C. M., Frohlich, H.-J., Straube, U., & others. (2001). Optical studies of crystals. *Journal of Applied Physics, 90*(12), 6084–6088. https://doi.org/10.1063/1.1409574
[21] Zhang, N., Wu, J., & Zhang, H. (2025). Crystal structure and optical properties. *Crystals, 15*(3), 269. https://doi.org/10.3390/cryst15030269
[22] Stadnyk, V. Y., Romanyuk, M. O., & Brezvin, R. S. (1997). Optical and electronic parameters of $RbNH_4SO_4$ crystals. *Ferroelectrics, 192*(1–4), 203–207. https://doi.org/10.1080/00150199708216190
[23] Andriyevsky, B., Ciepluch-Trojanek, W., Stadnyk, V., Tuzyak, M., Romanyuk, M., & Kurlyak, V. (2007). Band structure and optical spectra of $RbNH_4SO_4$ crystals. *Journal of Physics and Chemistry of Solids, 68*(10), 1892–1896. https://doi.org/10.1016/j.jpcs.2007.05.017
[24] Stadnyk, V. Y. (1998). Baric changes of optical indicatrix of $RbNH_4SO_4$ crystals [in Ukrainian]. *Ukrainian Journal of Physics, 43*(2), 213–218.
[25] Stadnyk, V., Vyshnevskyi, V., Matviishyn, I., Baliha, V., & Lys, R. (2025). Refractometry of uniaxially compressed Rb_2SO_4 crystals. *Electronics and Information Technologies*,30, 177–186. https://doi.org/10.30970/eli.30.14
[26] Clark, S. J., Segall, M. D., Pickard, C. J., Hasnip, P. J., Probert, M. I. J., Refson, K., & Payne, M. C. (2005). First principles methods using CASTEP. *Zeitschrift für*

Kristallographie – Crystalline Materials, 220(5–6), 567–570. https://doi.org/10.1524/zkri.220.5.567.65075
[27] Hohenberg, P., & Kohn, W. (1964). Inhomogeneous electron gas. *Physical Review, 136*(3B), B864–B871. https://doi.org/10.1103/PhysRev.136.B864
[28] Kohn, W., & Sham, L. J. (1965). Self-consistent equations including exchange and correlation effects. *Physical Review, 140*(4A), A1133–A1138. https://doi.org/10.1103/PhysRev.140.A1133
[29] Hamann, D. R., Schlüter, M., & Chiang, C. (1979). Norm-conserving pseudopotentials. *Physical Review Letters, 43*(20), 1494–1497. https://doi.org/10.1103/PhysRevLett.43.1494
[30] Monkhorst, H. J., & Pack, J. D. (1976). Special points for Brillouin-zone integrations. *Physical Review B, 13*(12), 5188–5192. https://doi.org/10.1103/PhysRevB.13.5188
[31] Perdew, J. P., Burke, K., & Ernzerhof, M. (1996). Generalized gradient approximation made simple. *Physical Review Letters, 77*(18), 3865–3868. https://doi.org/10.1103/PhysRevLett.77.3865
[32] Pfrommer, B. G., Côté, M., Louie, S. G., & Cohen, M. L. (1997). Relaxation of crystals with the quasi-Newton method. *Journal of Computational Physics, 131*(1), 233–240. https://doi.org/10.1006/jcph.1996.5612
[33] Perdew, J. P., Ruzsinszky, A., Csonka, G. I., Vydrov, O. A., Scuseria, G. E., Constantin, L. A., Zhou, X., & Burke, K. (2008). Restoring the density-gradient expansion for exchange in solids surfaces. *Physical Review Letters*, *100*(13), 136406. https://doi.org/10.1103/PhysRevLett.100.136406
[34] Råsander, M., & Moram, A. M. (2015). On the accuracy of commonly used density functional approximations in determining the elastic constants of insulators and semiconductors. *The Journal of Chemical Physics*, *143*(14), 144104. https://doi.org/10.1063/1.4932334
[35] Yuk, S. F., Sargin, I., Meyer, N., Krogel, J. T., Beckman, S. P., & Cooper, V. R. (2024). Putting error bars on density functional theory. *Scientific Reports*, *14*(1), 20219. https://doi.org/10.1038/s41598-024-69194-w
[36] Andrievsky, B., Jaskolski, M., Stadnyk, V., & others. (2013). Electronic structure calculations. *Computational Materials Science, 77*, 442–448. https://doi.org/10.1016/j.commatsci.2013.06.048
[37] Stadnyk, V., Gaba, V., Andrievskii, B., & Kogut, Z. (2011). Birefringence properties of mechanically clamped K_2ZnCl_4 crystals. *Physica Status Solidi B, 248*(1), 131–137. https://doi.org/10.1134/S106378341101029X
[38] Andrievsky, B., Romanyuk, M., & Stadnyk, V. (2009). Optical properties of materials. *Journal of Physics and Chemistry of Solids, 70*(7), 1109–1113. https://doi.org/10.1016/j.jpcs.2009.06.007
[39] Narasimhamurty, T. S. (1981). *Photoelastic and electro-optic properties of crystals*. Springer. https://doi.org/10.1007/978-1-4757-0025-1

ПРУЖНІ ВЛАСТИВОСТІ КРИСТАЛІВ $RbNH_4SO_4$

Олег Маркевич[1], Василь Стадник[1], Олег Бовгира[1], Роман Лис[2]*, Ігор Матвіїшин[2], Олег Онуфрів[3]
Львівський національний університет імені Івана Франка,
[1]Фізичний факультет, вул. Драгоманова 19, м. Львів, 79005, Україна,
[2]Факультет електроніки та комп'ютерних технологій,
вул. Генерала Тарнавського 107, м. Львів, 79017, Україна.
[3]Національний лісотехнічний університет,
вул. Генерала Чупринки 103, м. Львів, 79057, Україна

АНОТАЦІЯ

Вступ. Пружні властивості матеріалу є важливими для фізики твердого тіла, оскільки вони суттєво впливають на оптичні властивості кристалів.

Матеріали та методи. У роботі досліджено пружні властивості кристалів рубідій амоній сульфату $RbNH_4SO_4$. Розрахунок пружних властивостей проведено за допомогою програми CASTEP.

Результати. Аналіз матриці пружних коефіцієнтів $RbNH_4SO_4$ свідчить, що цей кристал належить до ромбічної сингонії із вираженою пружною анізотропією. Нерівність пружних констант вказує на складний характер міжатомних сил. Встановлено, що кристал є механічно стабільним, найбільша жорсткість є вздовж *Y* – напряму, найменша – вздовж *X*. Оскільки $C_{55} > C_{44} > C_{66}$, то найбільш стійкий зсув є в площині *XZ*, найменший – в площині *XY*. Розрахунок відношень Коші виявив значне відхилення ($C_{ij} > C_{kl}$), що вказує на переважання нецентральних сил у міжатомній взаємодії та наявність суттєвого внеску ковалентної або іонної складової зв'язку в ґратці $RbNH_4SO_4$.

У роботі розраховано просторовий розподіл модуля Юнга, модулі всебічного стискання, Юнга, зсуву та коефіцієнт Пуассона. Оцінено ступінь анізотропії пружних властивостей кристала $RbNH_4SO_4$, що підтверджує його значну анізотропію.

Висновки. Розрахунок критеріїв Борна показав, що кристал є механічно стабільним. Порівняння головних пружних коефіцієнтів показало, що найбільша жорсткість є вздовж *Y* – напряму, тоді як вздовж *X* – напряму вона є найменшою. Розрахунок відношень Коші виявив переважання нецентральних сил у міжатомній взаємодії та наявність суттєвого внеску ковалентної або іонної складової зв'язку в ґратці $RbNH_4SO_4$.

Наявність жорстких тетраедричних груп $[SO]_4^{2-}$ спричиняє утворенню ковалентниих напрямлених зв'язків всередині цих груп. Показано, що важливим є вплив поляризовності іонів: іони рубідію (Rb^+) та сульфатні групи $[SO]_4^{2-}$ мають велику електронну оболонку, яка деформується під час механічного стиснення кристалу. Це спричиняє виникнення індукованих дипольних моментів. Складний характер сил у кристалі $RbNH_4SO_4$ є наслідком того, що кристал складається не з точкових зарядів, а з поляризовних іонів та молекулярних комплексів $[SO]_4^{2-}$ із власним внутрішнім ковалентним зв'язком. Це робить матеріал пружно-анізотропним і чутливим до напрямку прикладеного навантаження.

Ключові слова: кристал, анізотропія, пружні коефіцієнти, модуль Юнга, модуль всебічного стискання, коефіцієнт Пуассона.

Received / Одержано	Revised / Доопрацьовано	Accepted / Прийнято	Published / Опубліковано
28 April, 2026	10 June, 2026	12 June, 2026	29 June, 2026